



Conversion of Ethanol to Diethyl acetal at Atmospheric Pressure over Cu/SBA-16 Catalysts

Gidyonu Paleti^{1,2}, Prathap Challa^{1,2}, Kamaraju Seetha Rama Rao¹
and David Raju Burri^{1*}

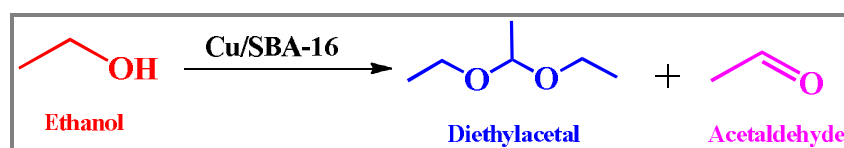
1. Catalysis and Fine Chemicals Division, CSIR-Indian Institute of Chemical Technology, Hyderabad-500007, **INDIA**
2. AcSIR-Academy of Scientific and Innovative Research, Gaziabad,-201002, **INDIA**
. Email: david.iict@gov.in

Accepted on 17th August, 2020

ABSTRACT

Copper nanoparticles in cage-like pores of SBA-16 were prepared by wet impregnation method and used in dehydrogenative reactions ethanol to commodity and specialty chemicals such as acetaldehyde and diethylacetal (DEE). The physicochemical features of the synthesized catalysts were characterized by X-ray diffraction, N₂-physisorption, SEM, TEM, temperature-programmed desorption of ammonia, TPR and N₂O pulse chemisorption. These analyses showed that Cu/SBA-16 catalysts maintained mesoporous structure of parent SBA-16 and that copper particles were highly dispersed in uniform pore channels of SBA-16. 24 wt% Cu/SBA-16 exhibited a maximum ethanol conversion of 62% and 63% selectivity to diethyl acetal. The superior catalytic activity in terms of conversion and selectivity during time on stream operation exhibited by Cu/SBA-16 catalyst is due to high dispersion and small particle sizes of Cu.

Graphical Abstract



Direct conversion of ethanol to diethyl acetal and acetaldehyde

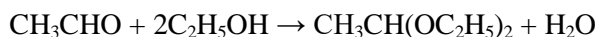
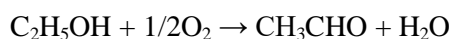
Keywords: Ethanol, Cu/SBA-16, Acetaldehyde, Diethyl acetal.

INTRODUCTION

The worldwide depletion of fossil resources has led to an increase in demand of renewable and sustainable alternatives for production of fuels, chemicals and energy. Although solar, wind, hydropower and geothermal power are all sources of renewable energy, biomass is the only largely accessible renewable source of carbon that is essential for the production of fuels and chemicals. Current industrial routes are almost entirely based on petroleum and other fossil resources [1]. Ethanol, derived from sugar fermentation, is the biofuel produced in largest volume from

renewable sources [2]. Although it is mainly used as fuel for combustion engines, ethanol has been studied as a possible raw material in the chemical industry, because it can be catalytically converted into several value-added chemicals by means of dehydration (to give ethylene), Guerbet coupling (n-butanol), dehydrogenation (acetaldehyde and hydrogen), by the coupling reaction of acetaldehyde with ethanol (ethylacetate) and by acetalization of acetaldehyde with ethanol (diethylacetal (DEE) and other chemicals [3-9]. Ethanol dehydrogenation stands out by importance of the products hydrogen and acetaldehyde which can be used as an intermediate in the manufacture of acetic acid, acetic anhydride, ethyl acetate, butyraldehyde, crotonaldehyde and n-butanol [10].

Moreover, the acetalization reaction of acetaldehyde with ethanol further give diethylacetal, a significant chemical, and is used as a raw material in fragrance and pharmaceutical industries and also an important intermediate in the production of industrial chemicals such as alkyl vinyl ethers. It is also used as an organic solvent for cellulose and its derivatives, and used for the production of polyacetal resins that are employed in electronic components, televisions, cars and printers. Diethyl acetal is clearly a promising green oxygenate useful for diesel blending, which improves the cetane number, reduces emissions of particulate matter and NO_x, and also facilitates combustion without decreasing the ignition quality (G). The industrial production of diethyl acetal is a two-step process. Here, acetaldehyde in the first step is produced from ethanol by carrying out oxidative dehydrogenation or hydrolysis of ethylene oxide. The produced acetaldehyde is then used for the acetalization of ethanol to produce diethyl acetal [5].



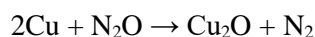
MATERIALS AND METHODS

SBA-16 preparation: SBA-16 was prepared according to procedure reported in literature by using triblock copolymer surfactant (EO106PO70EO106, called F127 (M/s. Sigma-Aldrich Chemicals, USA)) as a structure directing agent and tetraethyl orthosilicate (TEOS, M/s. Sigma Aldrich Chemicals, USA) as a silica source [11-13]. In a typical synthesis, 17.68 g of F127 was dissolved in 661.02 mL 0.5 M HCl at 313 K. After 3 h stirring, 85.71 mL of TEOS was added drop by drop. The solution containing a molar composition of 1 TEOS: 0.00367 F127: 0.864 HCl: 100.231 H₂O was stirred for 20 h at 313 K, and was subsequently transferred to a teflon bottle and aged at autogenous pressure for 24 h at 373 K. The material was filtered with several washings by using deionised water and dried at 373 K, and then calcined at 823 K for 6 h with a heating rate of 3 K min⁻¹ in air flow. The obtained solid was used as a support for the catalyst preparation.

Preparation of supported SBA-16 copper catalyst: Various Cu loaded (8, 12, 16, 20, 24 and 28 wt %) Cu/SBA-16 catalysts were prepared using wet-impregnation method with Cu(NO₃).6H₂O as Cu precursor. In a typical synthesis, the requisite amount of Cu precursor was dissolved in water; to this solution SBA-16 was added and it was heated on a hot plate at 353 K and kept in an oven at 373 K for 12 h. It was calcined in static air at 773 K for 5 h. The samples were labelled as xCS-16 where x represents weight percentage of Cu in Cu/SBA-16.

Characterization of catalysts: The amount of copper present in each catalyst sample was calculated using ICP-OES (M/s. Thermo Scientific iCAP6500 DU) by dissolving the Cu/SBA-16 catalyst sample in aquaregia with a few drops of HF (hydrofluoric acid). X-ray diffraction patterns of all the catalysts were obtained on an Ultima-IV (M/s. Rigaku Corporation, Japan) XRD unit which is operated at 40 kV and 40 mA equipped with nickel-filtered Cu K_α radiation (λ=1.54056 Å) and a 2θ value ranging from 0.7 to 80° at a scanning rate of 0.5 degree per min. BET specific surface areas, pore volumes and pore sizes were determined using N₂ physisorption studies (M/s. Quantachrome Instruments, USA) by

nitrogen adsorption at 77 K. Prior to measurement, the samples were degassed at 423 K for 2 h. The morphological studies of catalysts were carried out by scanning electron microscopy (M/s. JEOL, Switzerland) and TEM images were obtained on a JEM 2000EXII apparatus (M/s. JEOL, Switzerland) operating between 160 and 180 kV. Prior to TEM analysis, the catalyst sample was ultrasonicated in ethanol and a drop was placed onto a carbon coated copper grid; the solvent was then evaporated in an air oven at 353 K for 6 h. Temperature programmed reduction (TPR) was performed in laboratory-built equipment containing a quartz reactor with electrical heating and a gas chromatograph equipped with a thermal conductivity detector (TCD). About 100 mg of catalyst placed at the centre of the quartz reactor between two plugs of quartz wool was pre-treated at 573 K for 1 h in Ar flow (60 mL min⁻¹). Then the catalyst was exposed to 5% H₂ balance Ar gas flow for 1 h at 373 K followed by raising the temperature of the sample up to 1123 K at a heating rate of 10 K min⁻¹. The distributions of acidic sites were obtained from temperature-programmed desorption (TPD) of ammonia. A mass of about 50 mg of catalyst sample loaded in a sample tube was pre-treated in a flow of helium at 573 K for 30 min. Subsequently, the catalyst sample was saturated with a 10% NH₃/He gas mixture at 353 K for 30 min. After completion of saturation with NH₃, helium was allowed to flow for 30 min at 373 K for the removal of physisorbed NH₃. Helium gas flow was continued while increasing the temperature to 1073 K at a ramp of 10 K min⁻¹ and the desorbed NH₃ was monitored with an on-line GC equipped with TCD using standard GC software. N₂O pulse chemisorption measurements were taken using a home-made pulse chemisorption setup. An automatic gas sampling valve and a GC (GC-17A, M/s. Shimadzu Instruments Corporation, Japan) equipped with a TCD and Porapak-T column for separating N₂O and N₂ were connected at the inlet and outlet respectively. Prior to each experiment, the catalyst was reduced in an H₂ flow at 553 K for 3 h. After completion of the reduction, H₂ gas was replaced by helium gas (carrier gas for GC) and the temperature was brought down to room temperature, and N₂O gas (6% N₂O in helium) was introduced onto the catalyst in pulses using a 6-port valve. It was assumed that the surface Cu metal sites reacted with N₂O according to the stoichiometric equation



The copper metal surface area (Cu_{SA}) was calculated as the number of Cu moles g⁻¹ times Avogadro's number times the cross-sectional area of the copper metal. Here, the Cu cross sectional area was 6.8 × 10⁻²⁰ m² Cu atom⁻¹. The number of surface moles of Cu was calculated according to the expected stoichiometry to be 2 × N₂O uptake (mol g_{cat}⁻¹), and then used in the Dispersion equation

$$\text{Dispersion, \% D} = \left[\frac{\text{No. of surface Cu metal sites}}{\text{Total no. of metal sites in catalyst}} \right] \times 100$$

Catalytic activity test: Catalytic activity tests were performed in a fixed-bed glass down flow reactor at atmospheric pressure. For each catalytic run, the reactor was loaded with 0.5 g of the catalyst mixed with the same amount of glass beads sandwiched between two quartz wool plugs at the centre of the reactor. Prior to conducting the reaction, the catalyst was reduced for 3 h at 553 K. The reaction was carried out in the temperature range of 523–598 K by feeding ethanol into the reaction mixture at a flow rate of 1 mL h⁻¹ (feed pump, M/s. B. Braun, Germany) along with N₂ carrier gas. The product mixture was collected in an ice-cooled trap and analysed every 1 h using a GC-17A (M/s. Shimadzu Instruments, Japan) equipped with an FID and EB-5 capillary column (30 m × 0.53 mm × 5.0 μm). The products were confirmed by using a GC-MS (QP-2010, M/s. Shimadzu Instruments, Japan) with an MS column (30 m × 0.25 mm × 0.25 μm).

RESULTS AND DISCUSSION

The powder X-ray diffraction patterns of SBA-16 and Cu-SBA-16 samples were shown in [figure 1](#). From low angle (insert) XRD patterns, it can be observed that SBA-16, and copper nanoparticles

incorporated SBA-16 samples have retained their 3D pore arrangement, by exhibiting three diffraction peaks at 2θ values around 0.8° , 1.0° and 1.1° corresponding to the (110), (200) and (211) planes respectively, of regular mesoporous 3D cubic pore (Im3m) structure [11, 12]. The intensity of the (110) reflection decreases with increased copper loading. This phenomenon might be due to the partial loss of structural order or the reduced scatter contrasts between the pores and walls after loading metal particles in the pore channels of mesoporous silica. The wide-angle XRD patterns of all of the Cu/SBA-16 catalysts (Figure 1) exhibited a strong diffraction peak at $2\theta = 43.48^\circ$ and two more intense diffraction peaks at 50.5° and 74.1° characteristic of Cu° (JCPDS 04-0836), which indicated the presence of metallic Cu in all of the catalysts. Additionally, a broad hump was observed in each the XRD patterns of all of the catalysts at about 22° , which corresponded to amorphous silica of the SBA-16 support. The crystallite sizes marginally increased with increasing loading of Cu particles on the SBA-16 support (Table 1).

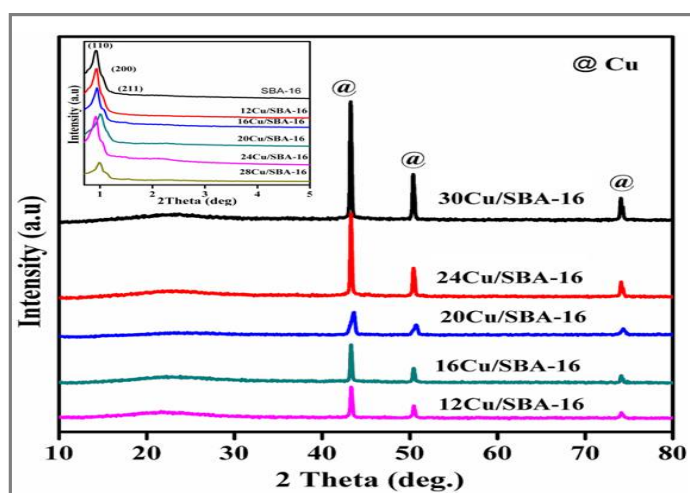


Figure 1. XRD patterns of reduced Cu/SBA-16 catalysts. Low-angle XRD patterns are shown in inset.

The N_2 adsorption-desorption isotherms of the samples are presented in figure 2. As shown in the figure, all the samples exhibited type IV isotherms with H1-type hysteresis loop as defined by IUPAC [11, 12]. This means that all catalysts have mesoporous structures. In addition, the surface area, pore volume, and pore diameter of synthesized catalysts are shown in table 1. The pore diameter of the samples was calculated from the NLDFT model of adsorption on Cu/SBA-15 (Table 1).

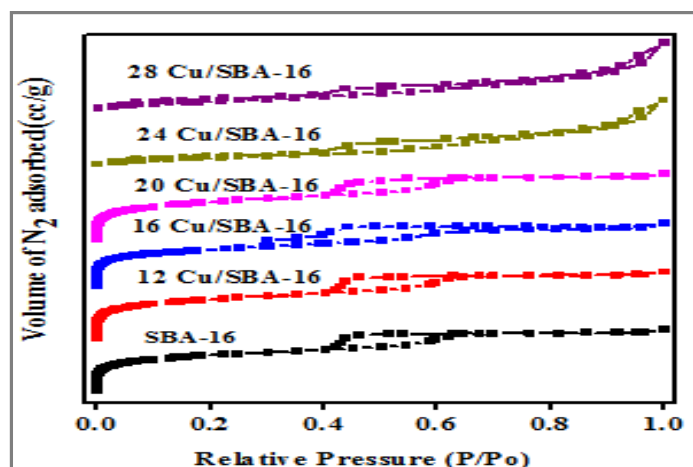


Figure 2. N_2 adsorption-desorption isotherms of SBA-15 and Cu/SBA-16 catalysts.

Table 1. Textural property measurements of the Cu/SBA-16 catalysts

Catalysts	S_{BET} ($\text{m}^2 \text{g}^{-1}$)	Pore volume (cc/g)	Pore diameter (nm)
SBA16	647	0.34	4.25
12Cu/SBA16	472	0.29	4.76
16Cu/SBA16	385	0.28	5.21
20Cu/SBA16	324	0.25	4.92
24Cu/SBA16	292	0.23	5.17
28Cu/SBA16	274	0.21	5.34

SEM and TEM images of the SBA-16 and 24 Cu/SBA-16 samples were depicted in figure 3. The morphology of the SBA-16 and 24 Cu/SBA-16 samples show agglomerated spheres like morphology typical of reported SBA-16 materials. It can be observed that 24Cu/SBA-16 sample is also maintaining the sphere like morphology even after copper incorporation in SBA-16. TEM images display the well ordered cubic pore structure in the SBA-16 and copper nanoparticles incorporation in SBA-16 sample. The results from the X-ray diffraction, N_2 physisorption and electron microscopic images suggest the maintenance of 3D mesoporous cubic arrangement in the SBA-16 and copper nanoparticles incorporated SBA-16 samples.

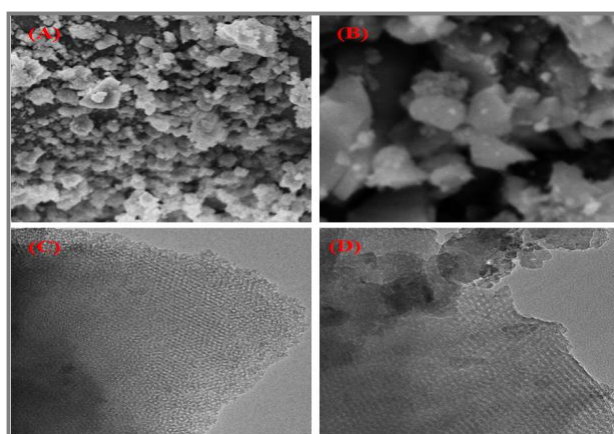


Figure 3. (A and B) SEM and (C and D) TEM images of (A and C) SBA-16 and (B and D) the 24Cu/SBA-16 catalyst.

To evaluate the reduction behaviour of CuO, the calcined CuO/SBA-16 catalysts were examined by H_2 -TPR and the resultant reduction profiles are shown in figure 4. The reduction profiles of Cu/SBA-16 show a single symmetric reduction peak. This reveals that CuO species present in the

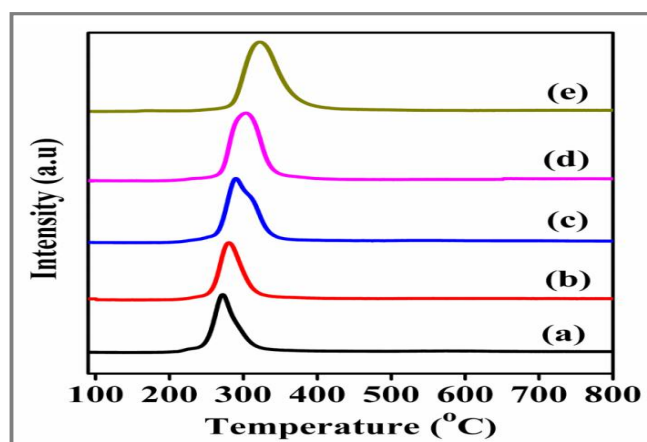


Figure 4. TPR profiles of Cu/SBA-16 catalysts. (a) 12Cu/SBA-16, (c) 16Cu/SBA-16, (d) 20Cu/SBA-16, (e) 24Cu/SBA-16 and (f) 28Cu/SBA-16 catalysts.

CuO/SBA-16 catalysts are reduced completely into Cu⁰ ($\text{CuO} + \text{H}_2 \rightarrow \text{Cu} + \text{H}_2\text{O}$) in a single-step. However, there is a marginal shift in temperature maxima towards higher temperatures from 271 to 323°C with increase in Cu loading on the SBA-16 support, indicating the attainment of bulk CuO with increase in Cu loading.

The NH₃ desorption profiles of SBA-16 and the Cu/SBA-16 catalysts are depicted in figure 5. The acidic sites can be classified depending upon the ammonia desorption temperature as weakly (<250°C), moderately (250-450°C) and strongly acidic sites (>450°C). The desorption signals observed in the TPD profile of pure SBA-16 can be ascribed to the surface hydroxyl groups. All of the catalysts except SBA-16 showed a desorption peak in the temperature range 130-250°C, indicating the weakly chemisorbed NH₃ molecules corresponding to the presence of a high quantity of weakly acidic sites arising from the dispersed copper. Another small peak at about 380 °C was observed, and was attributed to the presence of moderately acidic sites. From the total acidity values, the acidity of the catalyst increased linearly with the copper loading.

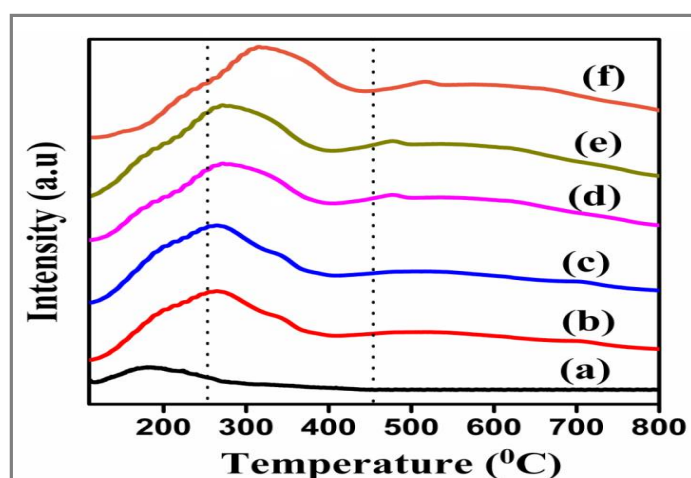


Figure 5. TPD of NH₃ profiles of Cu/SBA-16 catalysts. (a) SBA-16 support, and (b) 12Cu/SBA-16, (c) 16Cu/SBA-16, (d) 20Cu/SBA-16, (e) 24Cu/SBA-16 and (f) 28Cu/SBA-16 catalysts.

Table 2. N₂O chemisorption characteristics of the Cu/SBA-16 catalysts

Catalysts	^a Cu (nm)	^b Cu (wt%)	N ₂ O uptake (μmol/g)	^c Cu _{SA} (m ² /g)	^d Cu _D (%)	^e Cu _{PS} (nm)
12 CS-16	12.1	11.8	98.2	8.1	10.4	10
16 CS-16	13.2	15.2	117	9.64	9.3	11.2
20 CS-16	14.4	18.6	134.8	11.2	8.6	12.1
24 CS-16	15.2	22.9	148.2	12.2	7.8	13.2
28 CS-16	16.5	27.1	160	13.0	7.2	14.5

^aCrystallite size from XRD; ^bCu wt% from ICP-OES; ^cActive metal surface area; ^dCu dispersion; ^eCu particle size.

To estimate the copper metal surface area, dispersion and particle size, N₂O pulse chemisorptions were conducted and the acquired data are presented in table 2. The active Cu metal surface area and Cu metal particle sizes of Cu/SBA-16 catalysts were increased with amount of Cu content. To investigate the optimum quantity of Cus to load on the SBA-16 support, the direct conversion of ethanol to diethyl acetal was conducted on all six catalysts (12 Cu/SBA-15 to 28 Cu/SBA-16 catalysts) in the gas phase at 300°C in an inert atmosphere using nitrogen gas, and the corresponding data are displayed in figure 6. An increase in the percent conversion of ethanol was found with an increase in Cu loading from 12 to 24%, and this result was due to an increase in the number of active sites available for participating in the reaction. However, as the loading was further increased to 28%, no significant additional increase in conversion was observed, implying that such a high metal content may have led to agglomeration of Cu particles; furthermore,

selectivity in producing just diethyl acetal decreased significantly, due to the simultaneous increase in the producing other compounds (acetaldehyde, butanol and ethyl acetate).

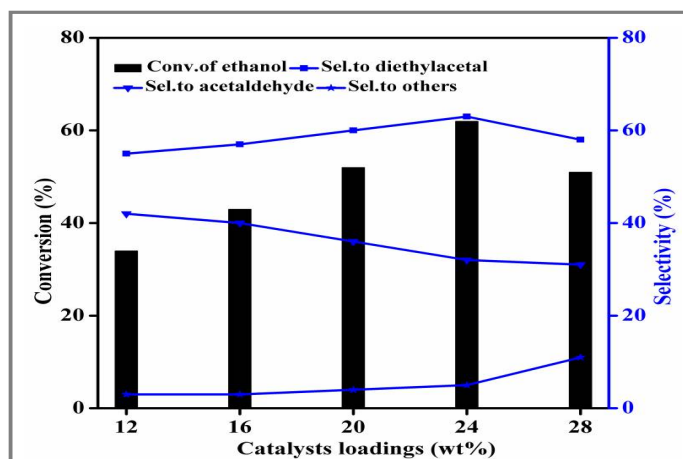


Figure 6. Effect of Cu loading on catalytic activity. Reaction conditions: temperature:300°C, catalyst weight: 0.5 g, N₂ flow: 30 mL min⁻¹, feed flow: 1 mL h⁻¹.

In order to determine the effect of reaction temperature on the activity of the 24 Cu/SBA-16 catalyst, the direct conversion of ethanol to acetaldehyde and diethylacetal (DEE) was conducted at five different temperatures, from 260 to 320°C (Figure 7). As the reaction temperature was increased from 260 to 300°C, the conversion of ethanol increased from 47 to 62% and the selectivity for diethyl acetal increased from 54 to 63%. As the reaction temperature was increased above 300°C, the ethanol conversions as well as the selectivity for diethyl acetal were observed to decrease, and at the same time the relative amounts of by-products increased significantly. Since conversion of ethanol to acetaldehyde is a primary step, its further conversion to diethyl acetal is an equilibrium reaction and, with increased temperatures, the promotion of the reverse reaction has been commonly found and increased formation of by-products was indeed expected.

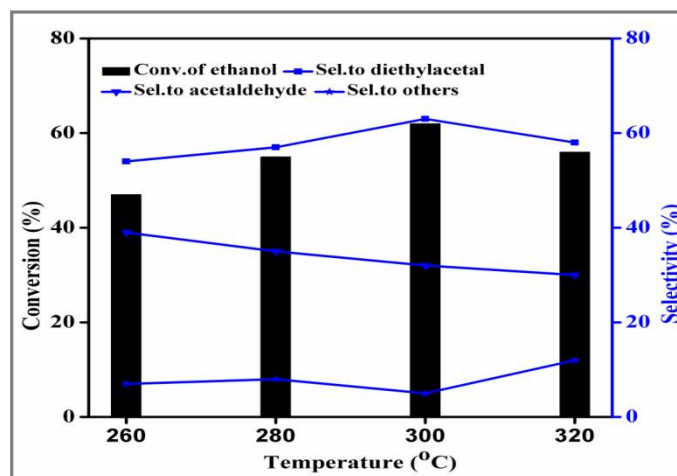


Figure 7. Effect of reaction temperature on activity of the 24 Cu/SBA-16 catalyst. Reaction conditions: catalyst weight: 0.5 g, N₂ flow: 30 mL min⁻¹, feed flow: 1 mL h⁻¹.

In order to explore the efficiency of 24 Cu/SBA-16 catalyst, a time-on-stream study was conducted on the 24 Cu/SBA-16 catalyst at 300°C for a period of 8 h. The conversion of ethanol and selectivity to diethyl acetal were constant at 62% and 63%, respectively (Figure 8), revealing that the activity of the catalyst was stable under the employed reaction conditions.

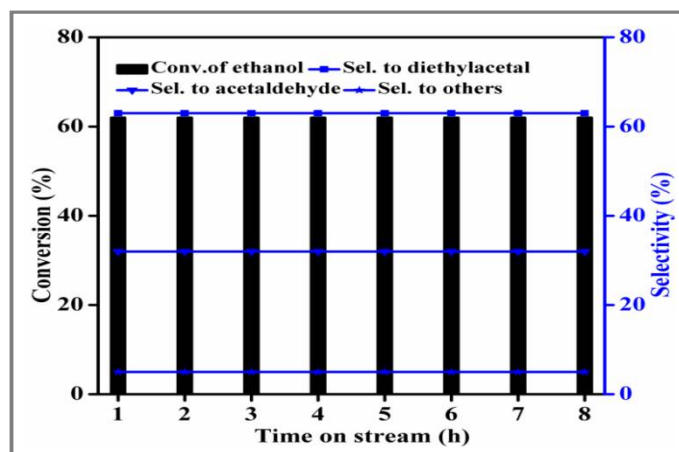


Figure 8. Time-on-stream activity of the 24Cu/SBA-16 catalyst. Reaction conditions: temperature: 300°C, catalyst weight: 0.5 g, N₂ flow: 30 mL min⁻¹, feed flow: 1 mL h⁻¹.

APPLICATION

The present work demonstrates the direct production of diethyl acetal and acetaldehyde from ethanol over Cu/SBA-16 catalyst instead of using toxic oxidants and reagents.

CONCLUSION

A series of Cu/SBA-16 catalysts were prepared by wet impregnation method and employed for direct conversion of ethanol to acetaldehyde and diethyl acetal in vapour phase at atmospheric pressure. All the SBA-16 supported Cu catalysts possessed parental mesoporous structure of SBA-16 even after a high amount of Cu (i.e. 28% wt.). Among Cu/SBA-16 catalysts, 24 Cu/SBA-16 catalyst offered better conversion of ethanol and selectivity to diethyl acetal in vapour phase at atmospheric pressure. The better activity is attributed to good dispersion of small Cu particles over high surface area SBA-16. 24 Cu/SBA-16 catalyst is stable in delivering constant activity during 8 h time-on-stream study.

REFERENCES

- [1]. A. Hommes, H. J. Heeres, J. Yue, Catalytic transformation of biomass derivatives to value-added chemicals and fuels in continuous flow microreactors, *Chem.Cat.Chem.*, **2019**, 11, 4671-470.
- [2]. C. Angelici, B. M. Weckhuysen, P. C. A. Bruijninx, Chemocatalytic conversion of ethanol into butadiene and other bulk chemicals, *ChemSusChem.*, **2013**, 6, 1595-1614,
- [3]. A. G.Sato , D. P.Volanti , D. M. Meira , S. Damyanova , E. Longo, J. M. CBueno, Effect of the ZrO₂ phase on the structure and behavior of supported Cu catalysts for ethanol conversion, *J. Catal.*, **2013**, 307, 1-17.
- [4]. A. G. Sato, D. P. Volanti, I. C. De Freitas, E. Longo, J. Maria, C. Bueno, Site-selective ethanol conversion over supported copper catalysts, *Catal. Commun.*, **2012**, 26, 122-126.
- [5]. G. Paleti, N. Peddinti, N. Gajula, V. Kadharabanchi, K. S. R. Rao, D. R. Burr, Direct ethanol condensation to diethyl acetal in the vapour phase at atmospheric pressure over CuNP/SBA-15 catalysts, *New J. Chem.*, **2019**, 43, 10003.
- [6]. E. V. Makshina, M. Dusselier, W. Janssens, J. Degrève, P. A. Jacobs, B. F. Sels, Review of old chemistry and new catalytic advances in the on-purpose synthesis of butadiene, *Chem. Soc.Rev.*, **2014**, 43, 7917-953.
- [7]. V. I. Sobolev, K. Koltunov, O. A. Simakova, A. R. Leino, D. Murzin, Low temperature gas-phase oxidation of ethanol over Au/TiO₂, *Appl. Catal. A.*, **2012**, 433-434, 88-95.

- [8]. T. Takei, N. Iguchi and M. Haruta, Synthesis of acetaldehyde, acetic acid, and others by the dehydrogenation and oxidation of ethanol, *Catal. Surv. Asia.*, **2011**, 15, 80 – 88.
- [9]. R. Prasad, Highly active copper chromite catalyst produced by thermal decomposition of ammoniac copper oxalate chromate, *Mater. Lett.*, **2005**, 59, 3945-3949.
- [10]. D. D. Petroilni, W.H. Cassinelli, C. A Pereira, E. A. Urquieta-Gonzalez, C. V. SantillL. Martins, Ethanol dehydrogenative reactions catalyzed by copper supported on porous Al–Mg mixed oxides, *RSC Adv.*, **2019**, 9, 3294.
- [11]. F. Kleitz, T. W. Kim, R. Ryoo, Phase domain of the cubic Im $\bar{3}$ m mesoporous silica in the EO₁₀₆PO₇₀EO₁₀₆–Butanol–H₂O system, *Langmuir*, **2005**, 22, 440.
- [12]. E. Siva Sankar, Ramesh G. V. Babu, Ch. Raji Reddy, B. David Raju, K. S. Rama Rao, Clean synthesis of alkyl levulinates from levulinic acid over one pot synthesized WO₃-SBA-16 catalyst, *J Mol Catal.,: A*, **2017**, 426, 30-38.
- [13]. S. Ganji, P. Bukya, Z. W. Liu, R. R. Kamaraju Seetha, D. R. Burri, Synthesis, spectroscopic studies and applications of CuNPs/SBA-15 catalysts, *J. Applicable Chem.*, **2019**, 8(3), 954-959.